

Pattern Synthesis for Slotted-Cylinder Antennas*

James R. Wait and James Householder

(June 11, 1959)

The radiation from a cylinder excited by an array of axial slots is discussed. A procedure for synthesizing a given radiation pattern is developed with particular attention being paid to a Tehebyseff-type pattern. Specifying the side lobe level and the width of the main beam, the required source distributions are computed for a number of cases. The effect of using a finite number of slot elements to approximate the continuous source distribution is also considered.

1. Introduction

It is the purpose of this communication to discuss the synthesis of radiation patterns for antennas of slotted-cylinder type. The particular model employed is a metallic cylinder of infinite length and perfect conductivity. The cylinder is to be energized by an array of slots of rectangular shape which are oriented in the axial direction and disposed around the circumference. Each slot is to be energized in such a way that the tangential field in the slot has only a transverse component. The radiation field of such a slot on an infinite cylinder is plane polarized. Furthermore, the idealization of an infinitely long cylinder is not overly restrictive since the surface currents excited by the axial slot are very similar to what they would be on a finite cylinder. This conjecture is substantiated by experimental data on the conductance of axial slots on finite cylinders [1].¹

2. Basic Pattern Function

Choosing a cylindrical coordinate system (ρ, ϕ, z) , the cylinder is defined by $\rho = a$. Since attention is only confined to the azimuthal or ϕ behavior, it is only necessary to specify the ϕ variation of the field in the axial slot. For example, if the slot width extends from ϕ_1 to ϕ_2 , the azimuthal radiation pattern $M^*(x, \phi)$ was shown to be given by [1]

$$M^*(x, \phi) = \frac{1}{i\pi x} \sum_{m=0}^{\infty} \frac{\epsilon_m e^{im\pi/2} \cos m\phi}{H_m^{(2)'}(x)} J_0\left(\frac{\phi_2 - \phi_1}{2} m\right), \quad (1)$$

where $H_m^{(2)'}(x)$ is the derivative with respect to x of the Hankel function of order m , J_0 is the Bessel function of order zero, $k = 2\pi/\text{wavelength}$, $x = ka \sin \theta$, $\epsilon_0 = 1$, $\epsilon_m = 2$ ($m \neq 0$), and θ is the angle subtended by the cylinder or z axis and the direction to the observer (i. e., the usual polar angle in spherical coordinates).

The above form for the pattern $M^*(x, \phi)$ is strictly valid only when the field E_ϕ in the slot is

$$E_\phi(\phi_0) = \frac{V(z_1)}{a\pi\sqrt{(\Delta/2)^2 - \phi_0^2}}, \quad (\Delta = \phi_2 - \phi_1), \quad (2)$$

where $V(z_1)$ is the voltage across the slot at $z = z_1$. The field approaches infinity as the inverse square root of the distance to the edge of the slot. Such a behavior is characteristic of the field in the vicinity of a perfectly conducting knife edge.

The amplitude and normalized phase Φ [=phase $M^*(x, \phi) - x \cos \phi$] of the quantity $M^*(x, \phi)$ is calculated for a series of values of x and $\phi_2 - \phi_1$. These are listed in tables 1 and 2 for x equal to 3 and 5, respectively, and $\phi_2 - \phi_1$ varying from 0° to 30° . For the smaller cylinder, it is seen that the effect of widening the slot (for a given voltage) is small. For the larger cylinders, the effect is becoming more significant although if the angular slot width is also less than 10° , the pattern is indistinguishable from that of zero width.

It should be emphasized that these E -plane patterns characterize only the azimuthal dependence of the radiation field for a given value of $x (=ka \sin \theta)$. The elevation patterns or H plane pattern of such an axial slot requires that the longitudinal distribution of voltage along the slot be specified [1].

3. General Array Synthesis

By superimposing the patterns of individual axial slots arranged circumferentially around the cylinder, various forms of patterns can be obtained. The problem sometimes arises that a pattern is specified and the manner of excitation must be determined. This is described as synthesis. Some elegant procedures have been developed for linear arrays and these have been described extensively in the literature [2 through 5]. When the antennas are disposed around circular arcs, the techniques [6] are not so straightforward, particularly if diffraction is involved. An example falling in this category will be considered in what follows.

*The research reported in this paper was sponsored, in part, by the U.S. Air Force Cambridge Research Center under Contract CSO and A 58-40.

¹ Figures in brackets indicate the literature references at the end of this paper.

TABLE 1^a
(From reference [7])

		$x=3$			$\Phi(\text{deg})$		
$\phi_2 - \phi_1$	$ M^*(x, \phi) $			$\Phi(\text{deg})$			
	0	20	30	0	20	30	
$\phi = 0$	0.959	0.957	0.955	6.9	5.7	4.2	
10	.956	.953	.948	7.1	5.9	4.5	
20	.946	.937	.926	7.7	6.6	5.2	
30	.927	.909	.888	8.4	7.4	6.2	
40	.895	.869	.838	8.9	8.1	7.2	
50	.859	.824	.783	8.8	8.2	7.7	
60	.825	.782	.731	8.0	7.9	8.0	
70	.794	.743	.684	7.4	8.0	8.7	
80	.747	.691	.626	7.8	8.8	10.2	
90	.664	.609	.545	7.6	9.0	11.0	
100	.561	.512	.455	3.2	5.0	7.5	
110	.482	.445	.395	-7.0	-5.1	-2.0	
120	.470	.428	.379	-18.1	-15.4	-11.7	
130	.444	.404	.358	-23.5	-20.4	-16.1	
140	.349	.320	.283	-28.7	-23.9	-19.2	
150	.206	.187	.166	-43.5	-40.0	-35.2	
160	.155	.142	.126	-105.0	-101.7	-97.0	
170	.259	.237	.211	-137.0	-133.5	-128.6	
180	.312	.285	.254	-142.1	-138.5	-133.6	

^a All angles are shown in degrees.

TABLE 2^a
(From reference [7])

		$x=5$				$\Phi(\text{deg})$			
$\phi_2 - \phi_1$	$ M^*(x, \phi) $				$\Phi(\text{deg})$				
	0	10	20	30	0	10	20	30	
$\phi = 0$	0.981	0.980	0.979	0.979	4.9	4.5	2.8	0.2	
10	.977	.976	.970	.960	5.1	4.7	3.0	.5	
20	.966	.963	.945	.918	5.1	5.1	3.5	1.2	
30	.951	.944	.908	.855	5.8	5.5	4.1	2.3	
40	.936	.924	.865	.782	6.1	5.9	5.0	3.8	
50	.914	.899	.815	.701	7.0	6.9	6.4	6.2	
60	.865	.844	.745	.610	7.9	7.9	8.0	8.7	
70	.804	.781	.672	.527	7.0	7.1	7.9	10.1	
80	.757	.732	.615	.462	5.5	5.8	7.6	11.6	
90	.681	.656	.540	.392	5.0	5.4	8.0	13.7	
100	.570	.548	.447	.318	-0.6	0	3.4	10.5	
110	.513	.493	.400	.282	-11.3	-10.5	-6.2	2.7	
120	.452	.434	.350	.245	-17.5	-16.6	-11.6	-1.3	
130	.318	.306	.246	.172	-32.7	-31.8	-26.4	-15.3	
140	.288	.277	.224	.158	-68.0	-67.0	-61.4	-49.8	
150	.293	.281	.228	.162	-82.8	-81.7	-75.7	-63.5	
160	.147	.141	.114	.082	-99.7	-98.8	-92.6	-77.0	
170	.142	.137	.112	.080	-205.2	-204.0	-198.0	-185.7	
180	.241	.232	.189	.135	-219.3	-218.2	-212.1	-199.6	

^a All angles are shown in degrees.

The cylinder is now to have P axial slots equispaced around a circumference of the cylinder as illustrated in figures 1a and 1b. The individual slot elements are centered at

$$\phi = \phi_p = \frac{2\pi p}{P} \text{ where } p=0, 1, 2 \dots P-1.$$

The quantity $L(\phi_p)$ is used to describe the relative excitation of each element. Therefore, the resultant azimuthal pattern of the array is

$$\bar{M}(\phi) = \frac{1}{2\pi} \sum_{p=0, 1, 2, \dots}^{P-1} L(\phi_p) M^*(\phi - \phi_p) \quad (3a)$$

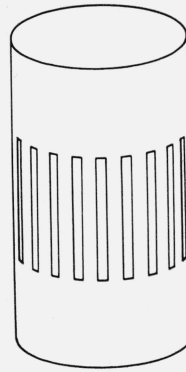


FIGURE 1a. The axial slot-ted-cylinder array.

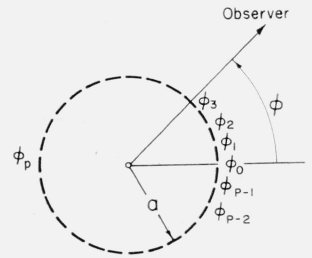


FIGURE 1b. Cross section of the cylinder.

where $M^*(\phi - \phi_p)$ is the pattern of the individual elements of the array. (The factor $1/2\pi$ is included for convenience in what follows.) Now when P is sufficiently large, $\bar{M}(\phi)$ can be approximated by an integral so that p is then regarded as a continuous variable. This leads to

$$\bar{M}(\phi) \cong \frac{1}{2\pi} \int_0^{2\pi} L(\phi_p) M^*(\phi - \phi_p) d\phi_p. \quad (3b)$$

It is now assumed that the excitation function $L(\phi_p)$ is expressible as a Fourier series in the manner

$$L(\phi_p) = \sum_{n=-\infty}^{+\infty} L_n e^{in\phi_p} \quad (4)$$

where the sum is over all integral values of n (including positive and negative integers). It is also assumed that the width of the individual slots is very small and therefore

$$M^*(\phi - \phi_p) \cong \frac{1}{i\pi x} \sum_{m=-\infty}^{+\infty} \frac{e^{im\pi/2} e^{im(\phi - \phi_p)}}{H_m^{(2)'}(x)} \quad (5)$$

which follows directly from eq(1). Inserting these expressions for $L(\phi_p)$ and $M^*(\phi - \phi_p)$ into eq(3b) leads to

$$\bar{M}(\phi) = \frac{1}{i\pi x} \sum_{m=-\infty}^{+\infty} \frac{L_m e^{im\pi/2} e^{im\phi}}{H_m^{(2)'}(x)}. \quad (6)$$

Having the pattern expressed in this form enables a synthesis procedure to be directly applied. Because of orthogonality

$$L_m = \frac{ix}{2} e^{-im\pi/2} H_m^{(2)'}(x) \int_0^{2\pi} \bar{M}(\phi) e^{-im\phi} d\phi \quad (7)$$

which, when inserted into eq(4), enables $L(\phi_p)$ to be determined and is the excitation required to produce the pattern $\bar{M}(\phi)$. In a formal sense, any pattern $\bar{M}(\phi)$ could be specified, however directive, and a corresponding function $L(\phi_p)$ could be determined. From a practical standpoint, there is a limitation

tern would not differ appreciably from the Tchebyscheff pattern. This conjecture is verified by actually computing the pattern for a finite number of equispaced slots disposed around the cylinder. For example, the polynomial $T_N(a \cos \phi + b)$ is to be compared with the function

$$\bar{M}(\phi) = \frac{1}{P} \sum_{p=0,1,2,\dots}^{P-1} L(\phi_p) M^*(\phi - \phi_p) \quad (17)$$

with P being a finite integer. In this case, the spacing between the axial slots is $2\pi a/P$. In spite of the fact that the spacing is finite, the $\bar{M}(\phi)$ pattern is quite close to the ideal T_N pattern as indicated in the following results.

4. Presentation of Numerical Results

The theoretical basis of the synthesis procedure has been outlined in the previous section. Here numerical results are presented for certain specific cases which illustrate the interrelation between the parameters of the problem.

The basic patterns used are illustrated in figure 2a and 2b. They are derived from the T_4 and T_6 polynomials, respectively. The quantity B , which is the (voltage) ratio of the major lobe to the minor lobe, is taken as 5, 10, 15, and 20 for the two cases. It is seen that for a given polynomial the beam is broadened as the side-lobe level is reduced. Consequently, if for a given side-lobe level, one wishes to

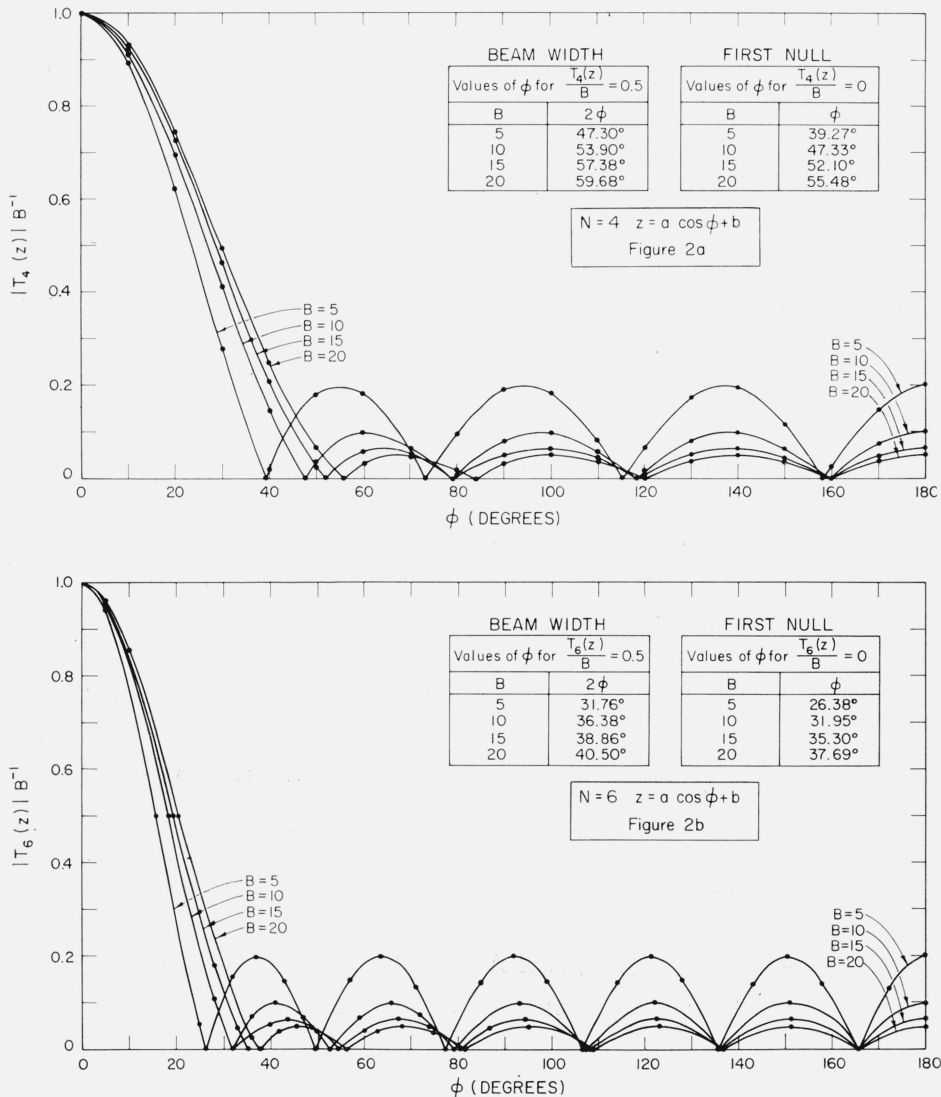
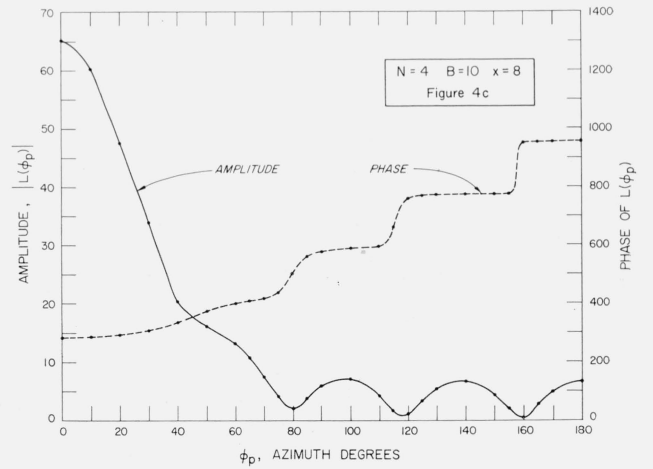
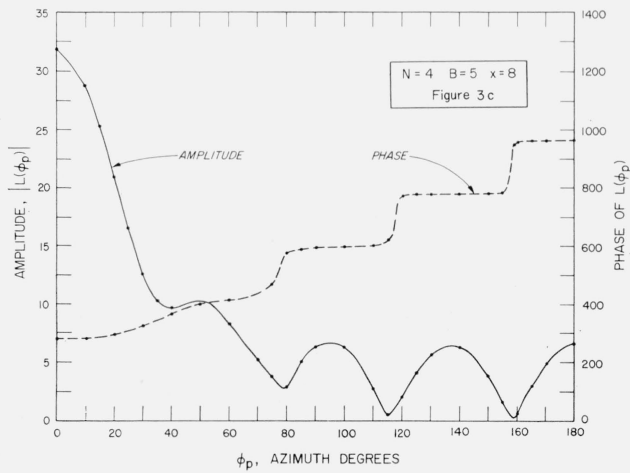
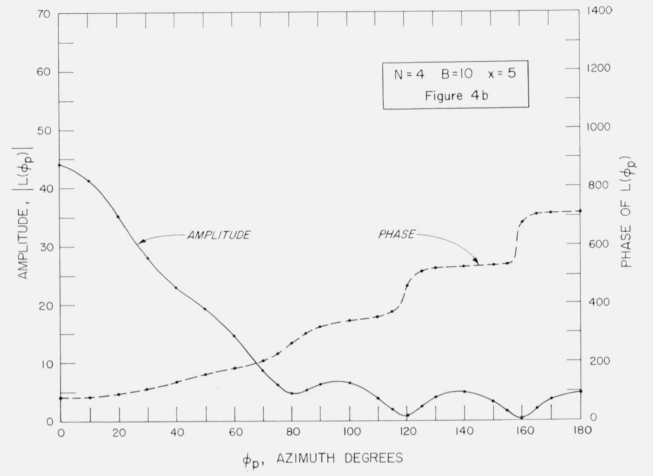
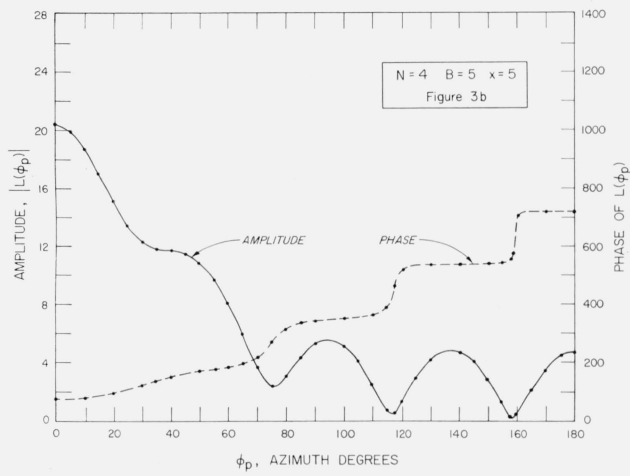
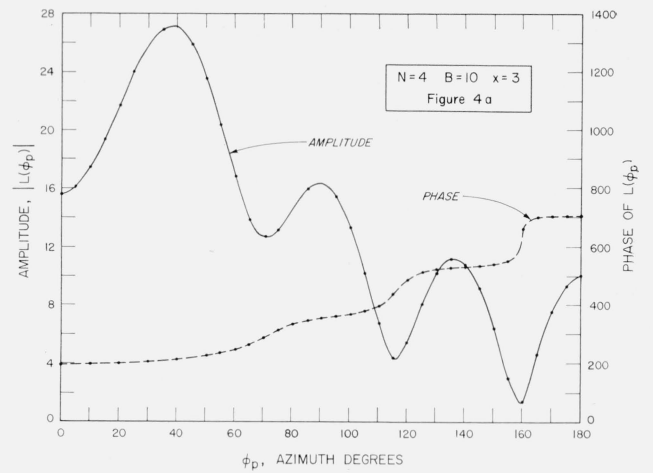
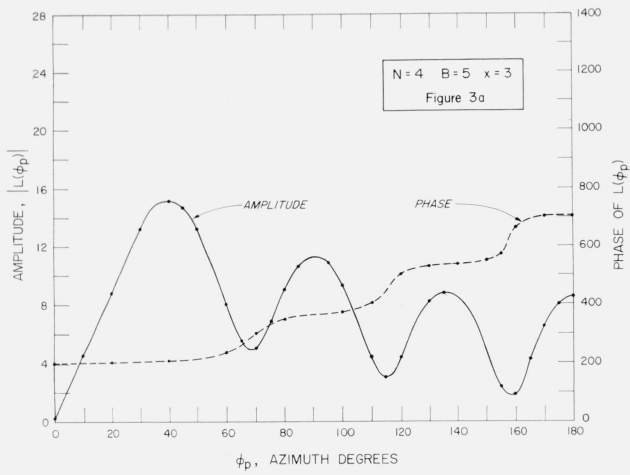
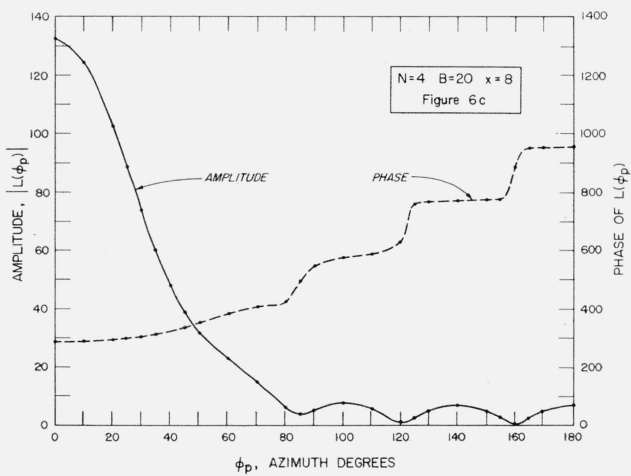
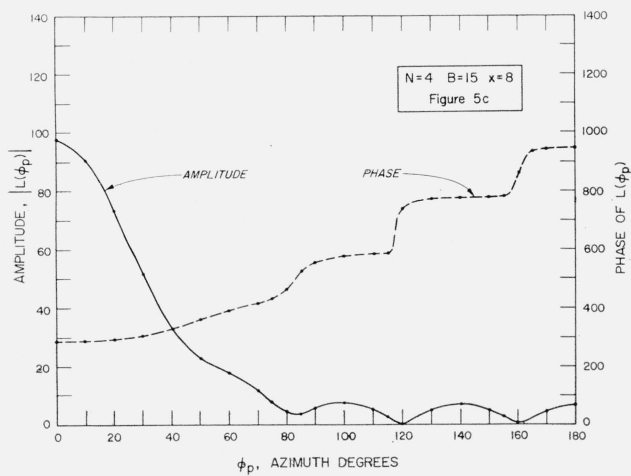
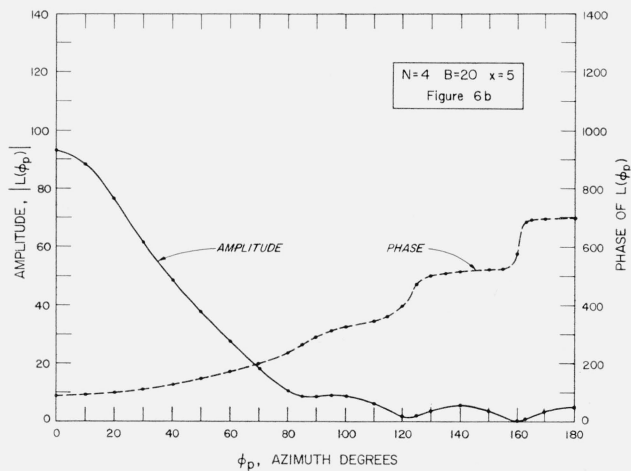
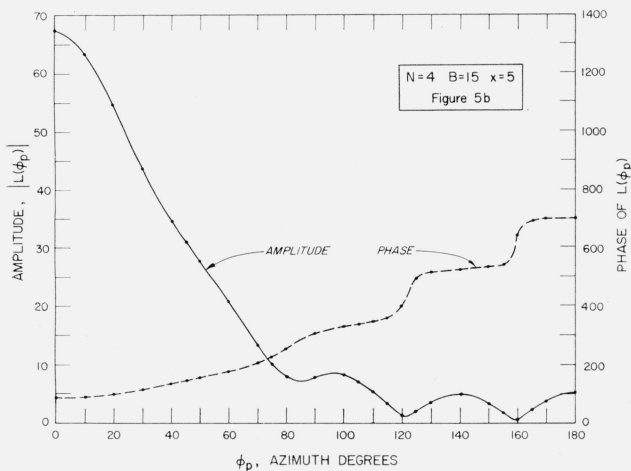
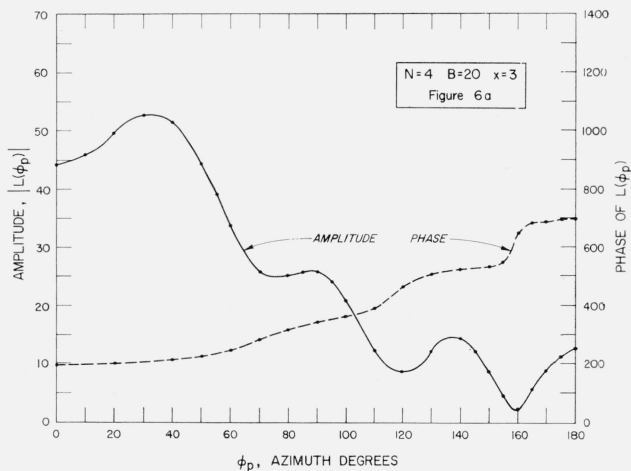
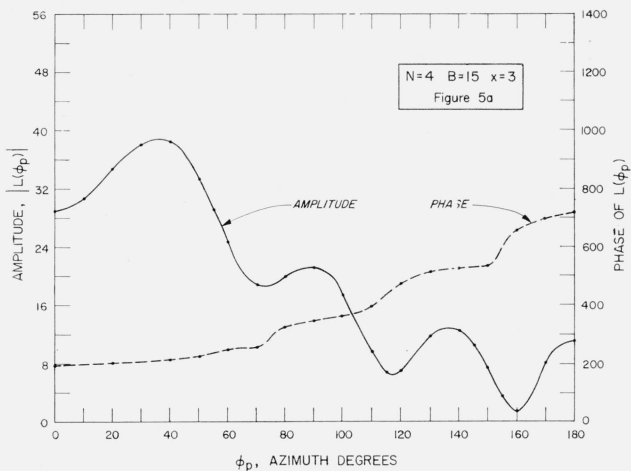


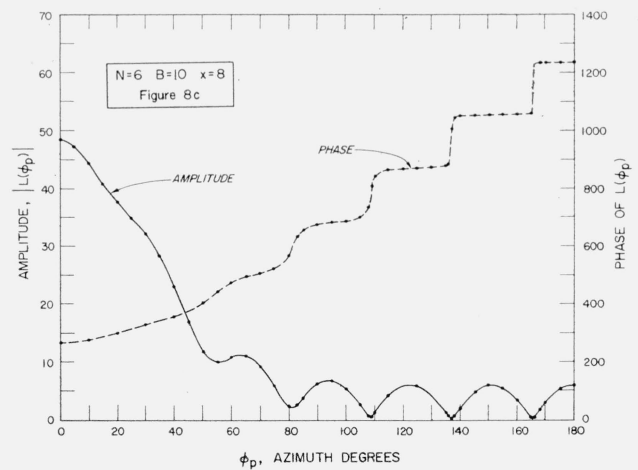
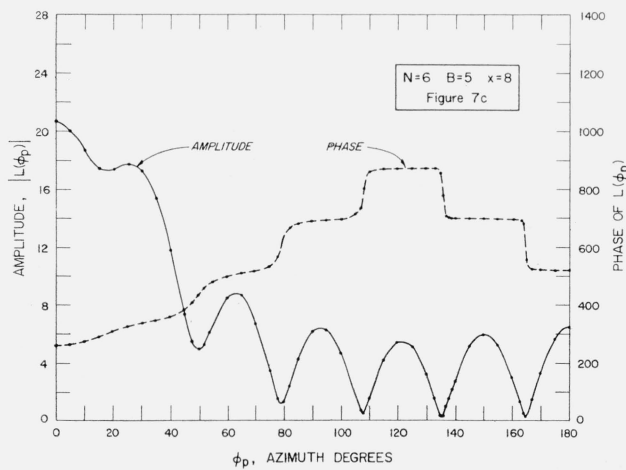
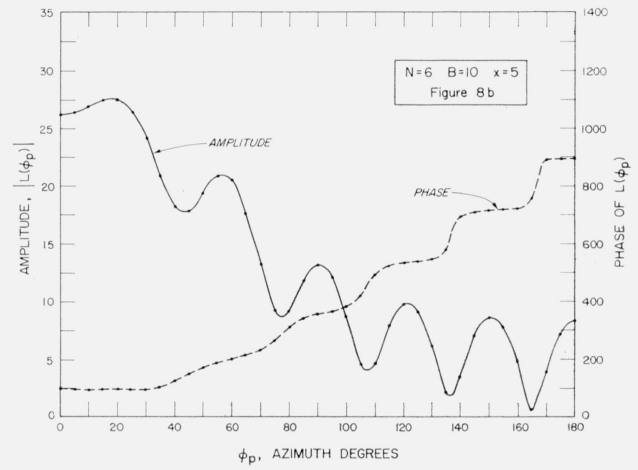
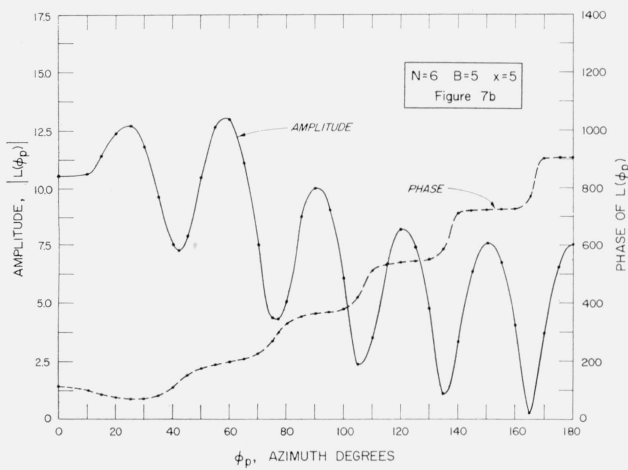
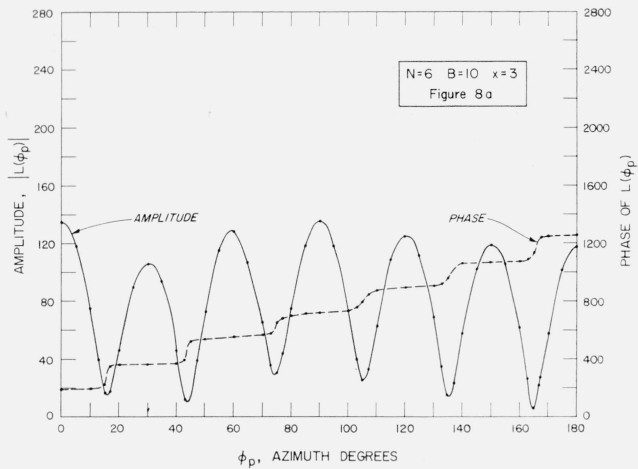
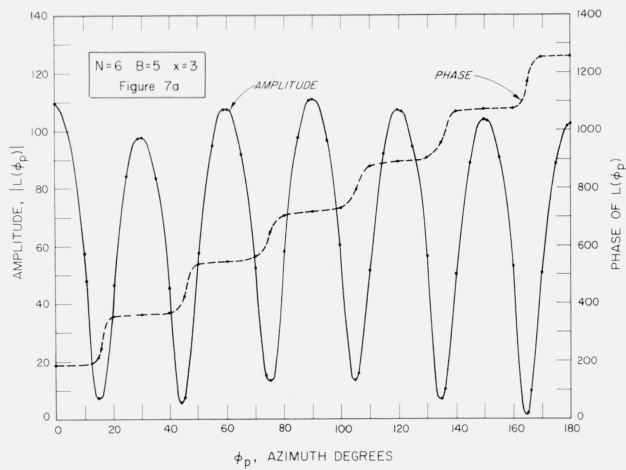
FIGURE 2. Optimum patterns based on Tchebyscheff polynomials $T_N(z)$.



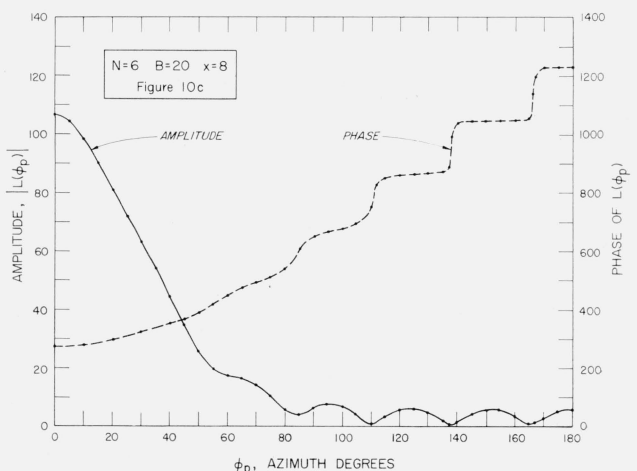
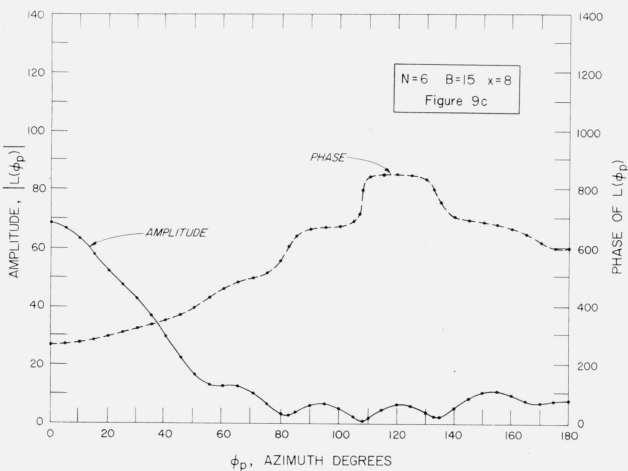
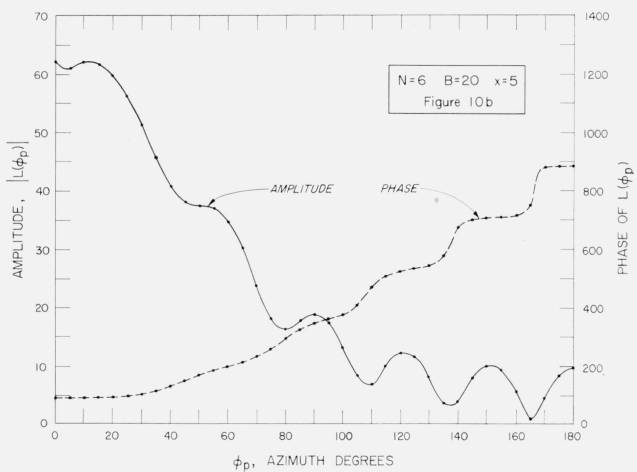
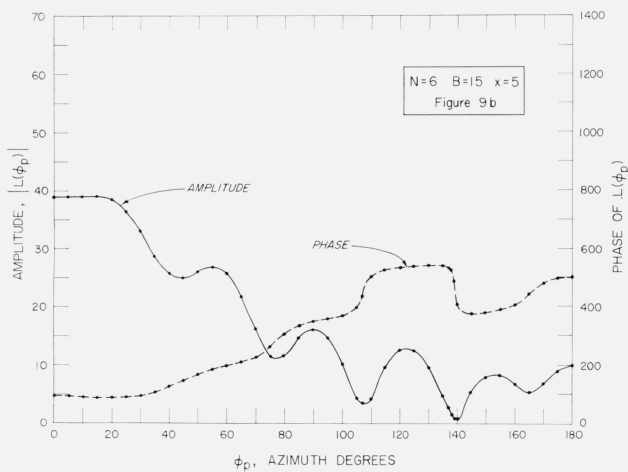
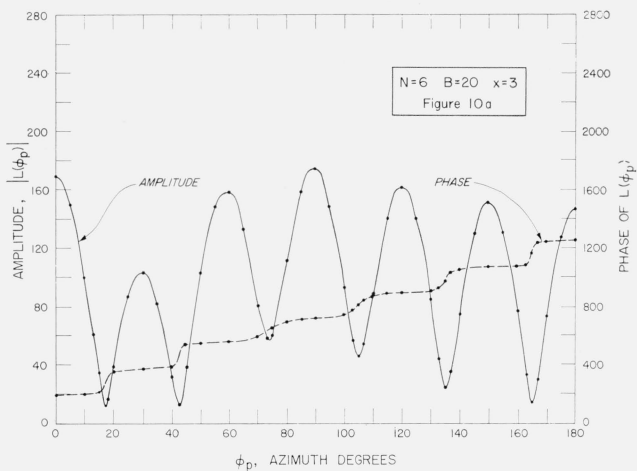
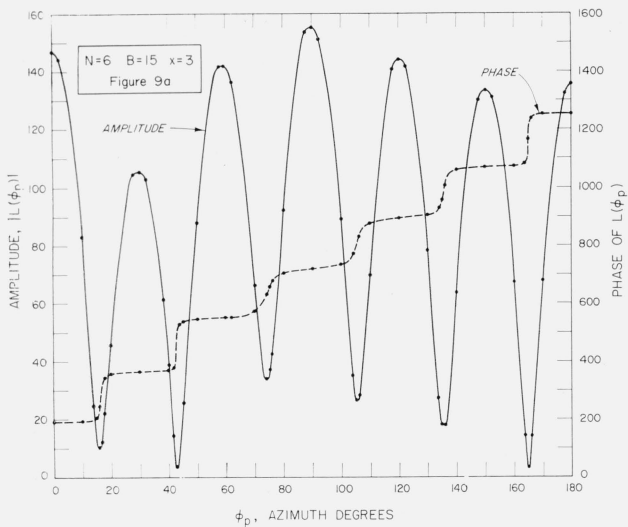
FIGURES 3 and 4. Excitation required for a Tchebyscheff pattern.



FIGURES 5 and 6. Excitation required for a Tchebyscheff pattern.



FIGURES 7 and 8. Excitation required for a Tchebyscheff pattern.



FIGURES 9 and 10. Excitation required for a Tchebyscheff pattern

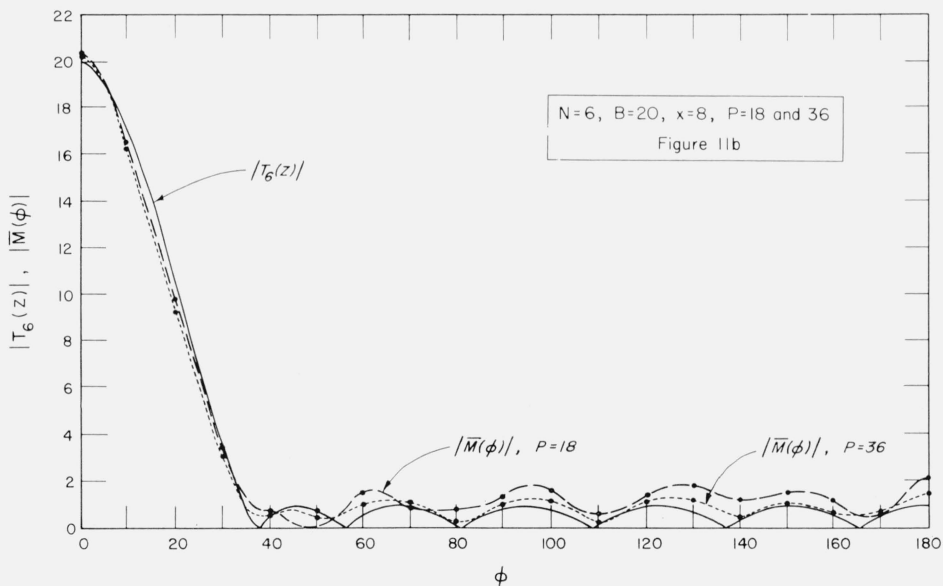
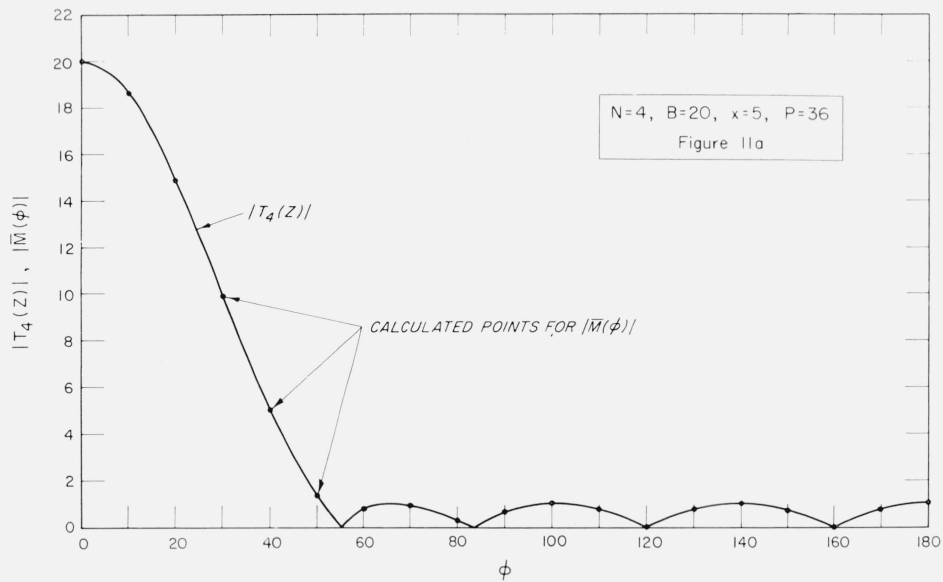


FIGURE 11. $|\bar{M}(\phi)|$ compared with $|T_N(z)|$.

reduce the beam width, a higher order polynomial must be employed. This fact is illustrated by noting that the beam width is narrower for the T_6 polynomial than for the T_4 polynomial for a given value of B .

The curves shown in figure 3a, 3b, 3c to figure 10a, 10b, 10c, inclusive, are plots of the amplitude and phase of the excitation function $L(\phi_p)$. The abscissas are the azimuthal coordinates ϕ_p expressed in degrees. On each figure is listed the relevant value of the order N of the Tchebyscheff polynomial, the lobe ratio B and cylinder parameter x .

It should be noted that the quantity x , which is $ka \sin \theta$, is fixed for each set of curves. In the equatorial plane (i.e., $\theta=90^\circ$) x becomes equal to ka which is the circumference of the cylinder in wavelengths.

In figure 7a (for $x=3$) it is noted that the excitation amplitude is varying in a very pronounced manner. Here, although the diameter of the cylinder is only about one-half wavelength, the main beam width is less than 32° . In figure 7b (for $x=5$) and figure 7c (for $x=8$), the oscillatory nature of the

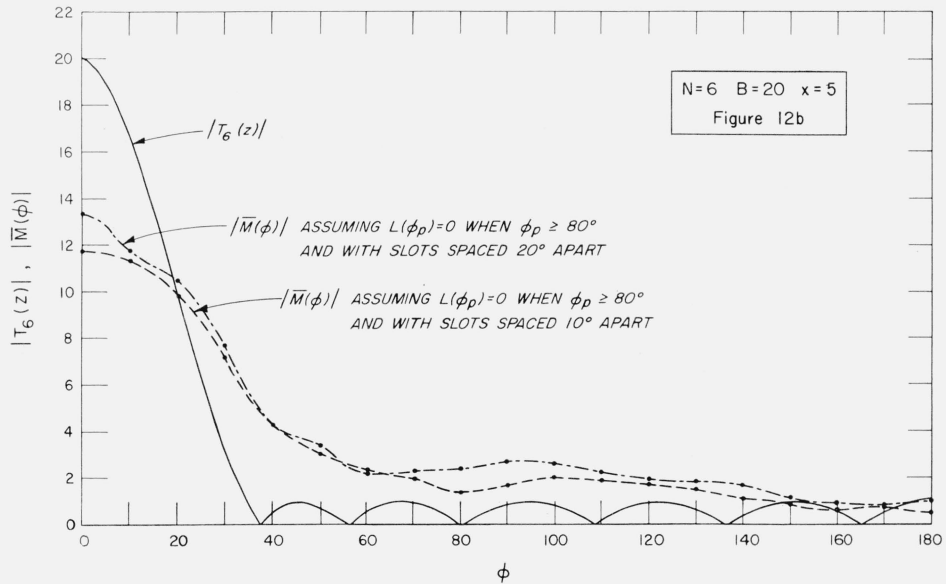
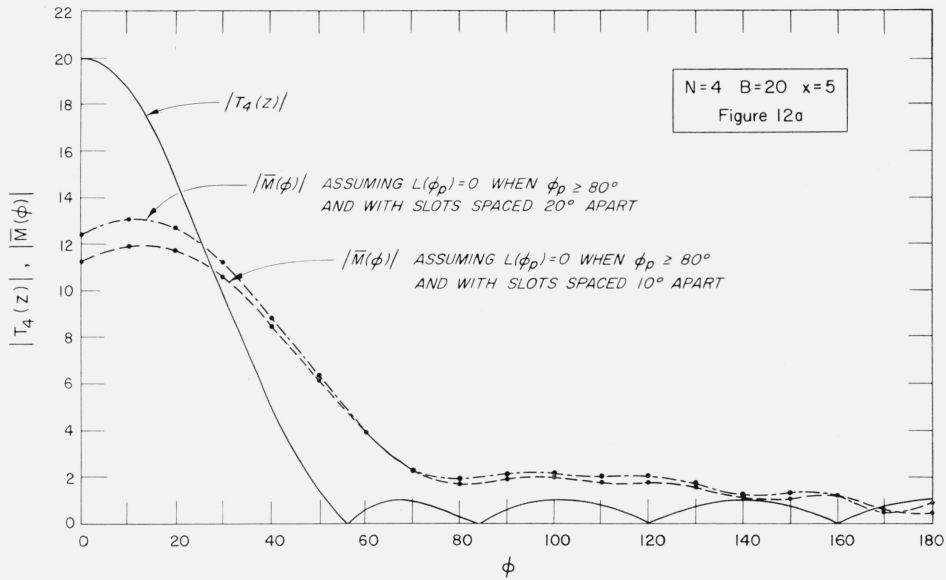


FIGURE 12. Pattern comparison for various assumptions.

excitation is less evident. The following sequence of figures for the larger B values show a similar trend.

In nearly every case shown in figure 3a to figure 10c, the phase of the excitation increases as ϕ_p ranges from 0° to 180° . When the amplitude is rapidly varying such as in figure 7a the phase increases almost abruptly by π radians (or 180°) near each minimum in the amplitude. There are several seemingly anomalous cases (fig. 7c, for example) where the π radian phase jump is down rather than up.

5. Effect of Using Discrete Sources

The excitation functions presented above are really descriptions of continuous source distributions. In a practical scheme it is usually necessary to approximate these by an array of discrete sources. As mentioned above, this is to be accomplished by an array of thin axial slots disposed uniformly around the circumference of the cylinder. In figure 11a is shown the pattern $|\bar{M}(\phi)|$ calculated from eq

(17) using 36 slots to approximate the continuous source distribution given by figure 6b. These calculated points lie virtually on top of the ideal Tchebyscheff (T_4) pattern. The apparent coincidence of the calculated and the ideal patterns is not surprising since the separation between the discrete sources is only $\frac{1}{2}$ of a wavelength, and thus the excitation is virtually a continuous one. A similar set of calculations are shown in figure 11b where the source distribution of figure 10c is approximated by both 18 and 36 discrete elements. There now appears to be some notable departures from the ideal Tchebyscheff pattern, particularly in the case for 18 elements where the side lobes are increased. In both cases, however, the main beam is preserved. In these two cases, the separation between the elements is $\frac{2}{9}$ and $\frac{1}{9}$ of a wavelength, so the degradation of pattern is not unexpected.

On examining some of the excitation functions (for example, fig. 6b), it is seen that on the rear half of the cylinder, the amplitude $|L(\phi_p)|$ is less than 10 percent of the maximum at $\phi_p=0$. As a matter of interest, the function $\overline{M}(\phi)$ was computed using eq (17) again, but now approximating $L(\phi_p)$ by discrete sources located only on a front portion of the cylinder (i. e., $|\phi_p| < 80^\circ$). Such results are shown in figure 12a for angular intervals between the slots of 10° and 20° . The computed pattern $\overline{M}(\phi)$ bears only a slight resemblance to the ideal T_4 pattern which would be closely simulated if the slots extended right around to the back of the cylinder. Similar calculations are shown in figure 12b where the excitation function shown in figure 10c is approximated by discrete sources on the front portion of the cylinder. Here again the pattern is considerably degraded from the ideal T_6 pattern although the increase of the side-lobe level may be tolerated for certain applications.

6. Concluding Remarks

It can be seen from the above curves that, in principle, any pattern may be obtained if the exci-

tation function or source distribution is specified in a certain way. Unfortunately, if narrow main beams are desired, the cylinder must be sufficiently large, otherwise very complicated excitation functions are required.

It appears that usually the continuous excitation or source function $L(\phi_p)$ can be approximated by discrete sources (i.e., narrow axial slots) if the separation is less than about $\lambda/8$. However, the rapidly varying excitation functions associated with small cylinders and narrow beams would require smaller spacing between the source elements.

7. References

- [1] J. R. Wait, Electromagnetic radiation from cylindrical structures (Pergamon Press, 1959); and J. R. Wait, Radiation characteristics of axial slots on a conducting cylinder, *Wireless Eng.* **32** 316 (1955).
- [2] C. L. Dolph, A current distribution for broadside arrays which optimizes the relationship between beam width and side lobe level, *Proc. IRE* **34** 335 (1946).
- [3] H. J. Riblet, Discussion of Dolph's Paper, *Proc. IRE* **35** 489 (1947).
- [4] G. Sinclair and F. V. Cairns, Optimum patterns for arrays of non-isotropic sources, *IRE Trans. PGAP-1*, 50 (1952).
- [5] R. H. Duhamel, Optimum patterns for end-fire arrays, *Proc. IRE* **41** 652 (1953).
- [6] R. H. Duhamel, Pattern synthesis for antenna arrays, Tech. Rept. No. 16, Elec. Eng. Research Lab. Univ. of Ill. (May 1952).
- [7] J. R. Wait and P. Wheelon, Further numerical results for the patterns of slotted-cylinder antennas, Rept. on Contract AF04 (645)-56 prepared by P.E.C. Corp. under the direction of D. G. Burkhard for the Martin Co. Denver Div. (June 1958).

Note added in proof:

A closely related problem has been studied by Adolf Giger in *On the Construction of Antenna Arrays with Prescribed Radiation Patterns*, doctoral thesis, Technischen Hochschule, Zurich, 1956. This was brought to our attention recently by Prof. Franz Tank.

BOULDER, COLO.

(Paper 63D3-27)